Supplementary Information for:

Bacterial SEAL domains undergo autoproteolysis and function in regulated intramembrane proteolysis

Anna P. Brogan[1], Cameron Habib[1], Samuel J. Hobbs[1,2], Philip J. Kranzusch[1,2], David Z. Rudner[1]*

[1]Department of Microbiology
Harvard Medical School
Boston, MA 02115

[2]Department of Cancer Immunology and Virology
Dana-Farber Cancer Institute
Boston, MA 02115

*rudner@hms.harvard.edu

List of Supplementary Materials:

Plasmid Construction
Figures S1-S13
Tables S1-S7
Uncropped gels and immunoblots

Plasmid Construction

pAB47 [His-SUMO-RsgI-S99A (amp)]
pAB47 was generated in a 2-piece isothermal assembly reaction using a PCR product amplified from pYB227 [amyE-sigI-rsgI (S99A) -S481-UTR (kan)(amp)] using oCH53 & oCH69 and pTD68 [His-SUMO (amp)] cut with BamHI.

pAB61 [yvbJ::PxylA-gfp-rsgI-His6 (erm)(amp)]
pAB61 was generated in a 2-piece isothermal assembly reaction using a PCR product amplified from PY79 gDNA with oAB112 & oAB113 and pYB200 [yvbJ::PxylA-gfp-His6 (erm)(amp)] cut with BamHI.

pAB66 [His-SUMO-RsgI(JMD)-S212A (amp)]
pAB66 was generated in a 2-piece isothermal assembly reaction using a PCR product amplified from pYB233[amyE-sigI-rsgI (S212A) -S481-UTR (kan)(amp)] using oCH53 & oCH69 and pTD68 [His-SUMO (amp)] cut with BamHI.

pAB67 [His-SUMO-RsgI-S99A-S212A (amp)]
pAB67 was generated in a 2-piece isothermal assembly reaction using a PCR product amplified from pYB227 [amyE-sigI-rsgI (S99A) -S481-UTR (kan)(amp)] using oCH53 & oAB117 and pTD68 [His-SUMO (amp)] cut with BamHI.

pAB78 [yvbJ::PxylA-gfp-rsgI-DI-GGG-NPS-His6 (erm)(amp)]
pAB78 was generated in a 3-piece isothermal assembly reaction using a PCR product amplified from PY79 gDNA with oAB112 & oAB128, a PCR product amplified using oAB113 & oAB129 and pYB200 [yvbJ::PxylA-gfp-His6 (erm)(amp)] cut with BamHI.

pAB79 [His-SUMO-RsgI(JMD)-DI-GGG-NPS (amp)]
pAB79 was generated in a 2-piece isothermal assembly reaction using a PCR product amplified from pAB78 with oCH53 & oCH69 and pTD68 [His-SUMO (amp)] cut with BamHI.

pAB87 [P_{T7}-GFP-RsgI(JMD) (amp)]
pAB87 was generated in a 3-piece isothermal assembly reaction using a PCR product amplified from pAB61 using oAB141 & oAB144, a PCR product amplified from PY79 gDNA using oAB142 & oAB143 and pDHFR (NEB) cut with NdeI and BamHI.

pAB90 [amyE::sigI-rsgI-DI-GGG-NPS-S481UTR (kan)(amp)]
pAB90 was generated in a 3-piece isothermal assembly reaction using a PCR product amplified from PY79 gDNA using oAB35 & oAB128, a PCR product amplified from P79 gDNA using oAB36 & oAB129, and pYB225 cut with NheI.

pAB93 [His-SUMO-HtRsgI2(JMD) (amp)]
pAB93 was generated in a 2-piece isothermal assembly reaction using a PCR product amplified from RsgI2 GBlock using oAB154 & oAB155 and pTD68 [His-SUMO (amp)] cut with BamHI.

pAB101 [P_{T7}-GFP-RsgI(JMD)-DI-GGG-NPS (amp)]
pAB101 was generated in a 3-piece isothermal assembly reaction using a PCR product amplified from pAB61 using oAB141 & oAB144, a PCR product amplified from pAB79 using oAB142 & oAB143, and pDHFR (NEB) cut with NdeI and BamHI.

pAB129 [amyE::sigI-rsgI-DI-GGG-NPS-ΔID-S481UTR (kan)(amp)]

pAB129 was generated in a 2-piece isothermal assembly reaction using a PCR product amplified from pAB90 using oAB35 & oYB425, and pYB225 cut with NheI.

pAB130 [yvbJ::PxylA-gfp-rsgI-DI-GGG-NPS-ΔID-His6 (erm)(amp)]
pAB130 was generated in a 2-piece isothermal assembly reaction using a PCR product amplified from pAB90 using oAB112 & oYB507, and pYB200 [yvbJ::PxylA-gfp-His6 (erm)(amp)] cut with BamHI.

pAB188 [His-SUMO-RsgI-GGG(JMD)-A88-S219 (amp)]
pAB188 was generated in a 2-piece isothermal assembly reaction using a PCR product amplified from pAB90 using oAB356 & oCH69, and pTD68 [His-SUMO (amp)] cut with BamHI.

pAB214 [His-SUMO-SEAL(*Dwelbionis*) (amp)]
pAB214 was generated in a 2-piece isothermal assembly reaction using a PCR product amplified from SEAL(D.welbionis) GBlock using oAB410 & oAB411, and pTD68 [His-SUMO (amp)] cut with BamHI.

pAB216 [His-SUMO-SEAL(*Pbrassicae*) (amp)]
pAB216 was generated in a 2-piece isothermal assembly reaction using a PCR product amplified from SEAL(Pbrassicae) using oAB412 & oAB413, and pTD68 [His-SUMO (amp)] cut with BamHI.

pCH26 [His-SUMO-CtRsgI(JMD) (amp)]
pCH26 was generated in a 2-piece isothermal assembly reaction using a PCR product amplified from *C. thermoalcaliphilum* gDNA using oCH63 & oCH54, and pTD68 [His-SUMO (amp)] cut with BamHI.

pCH27 [His-SUMO-HtRsgI4(JMD) (amp)]
pCH27 was generated in a 2-piece isothermal assembly reaction using a PCR product amplified from *H. thermocellum* gDNA using oCH65 & oCH66, and pTD68 [His-SUMO (amp)] cut with BamHI.

pCH29 [His-SUMO-BsRsgI(JMD) (amp)]
pCH29 was generated in a 2-piece isothermal assembly reaction using a PCR product amplified from PY79 gDNA using oCH53 & oCH69, and pTD68 [His-SUMO (amp)] cut with BamHI.

Figure S1
Brogan *et al.*

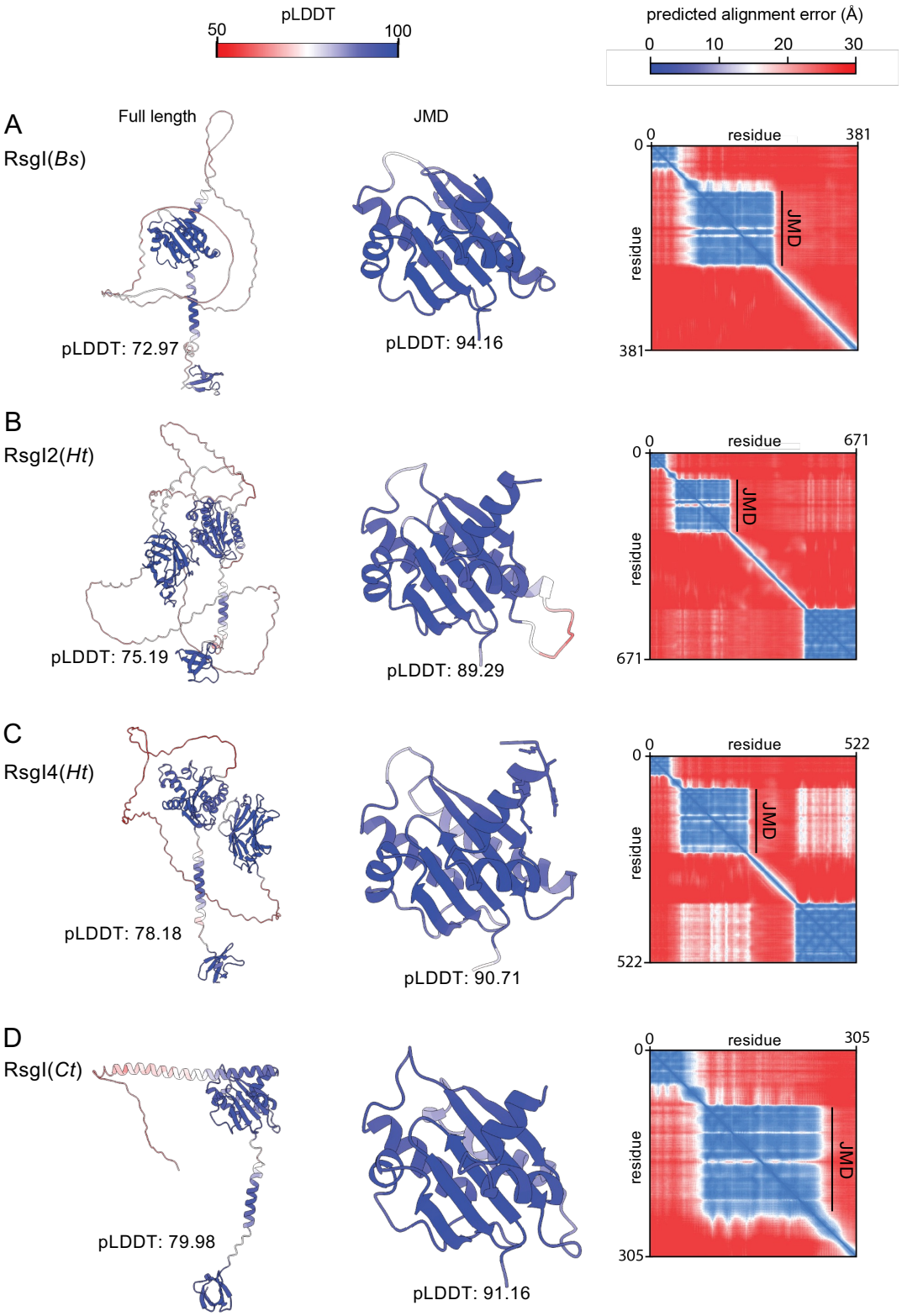

Figure S1. AlphaFold2 confidently predicts the juxtamembrane domain of RsgI homologs. AlphaFold-predicted structures colored by pLDDT, and pAE plots of **(A)** *B. subtilis* (*Bs*) RsgI; **(B)** *H. thermocellum* (*Ht*) RsgI2; **(C)** *H. thermocellum* RsgI4; and **(D)** *C. thermoalcaliphilum (Ct)* RsgI. The juxtamembrane domain (JMD) is highlighted on the pAE plots.

A

B

Length of Chain 1 (JMD)	133 residues
Length of Chain 2 (SEA)	107 residues
Aligned length	75 residues
RMSD	4.82 Å
SeqID	0.120
TMscore (normalized by chain 1)	0.30811
Tmscore (normalized by chain 2)	0.35229

Figure S2. RsgI's JMD and the SEA domain of MUC1 align by TM-align. (A) structural alignment of RsgI's JMD (purple) and MUC1's SEA domain (green). **(B)** Metrics for the domains and their alignment.

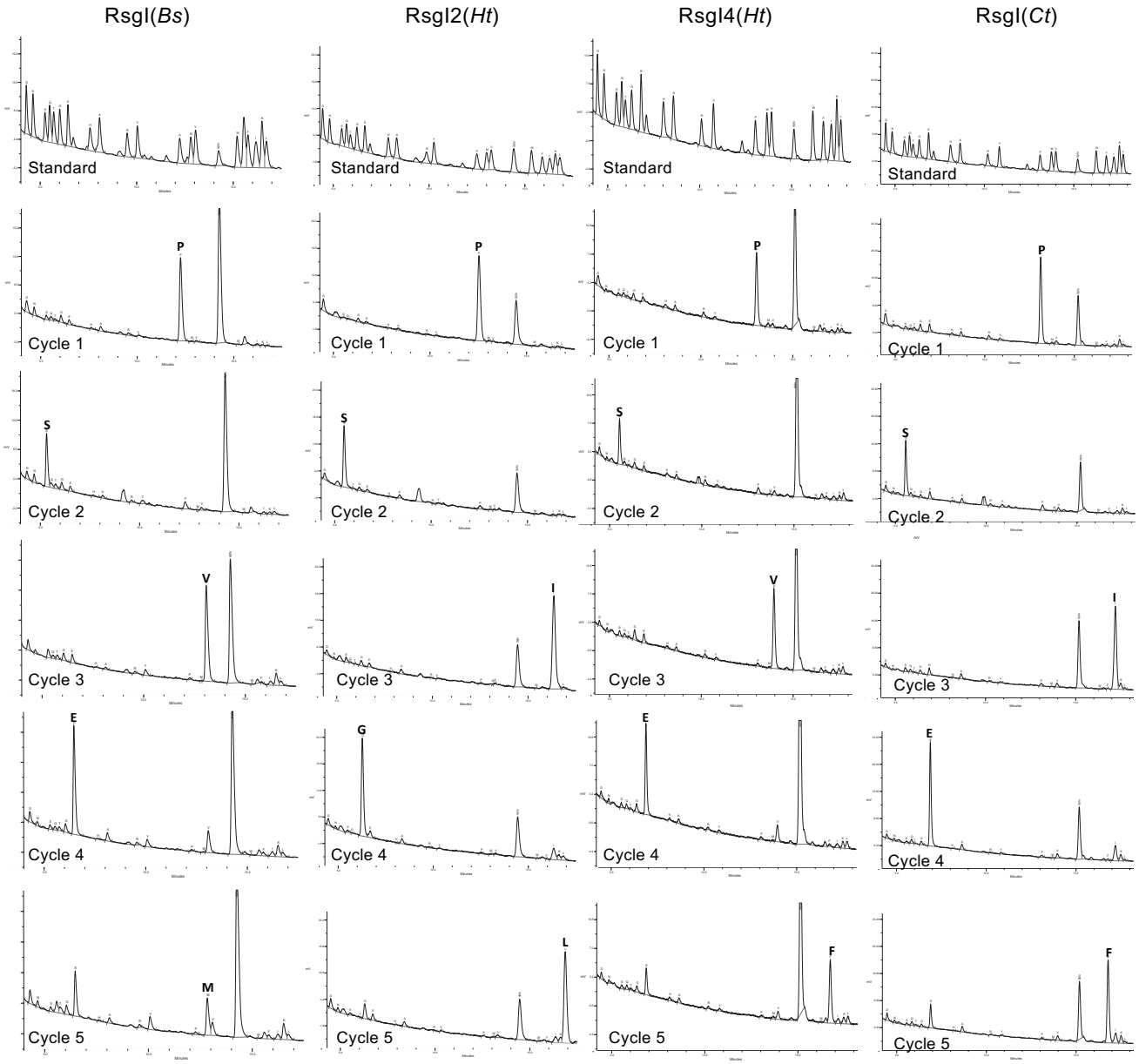

Figure S3. Edman degradation reveals a conserved cleavage site. Chromatograms from 5 cycles of Edman degradation for each of the four RsgI homologs tested as compared to standards of each amino acid. SEAL domains from each homolog were expressed and purified from *E. coli* and the N-terminal peptide sequence was determined from the C-terminal cleavage product.

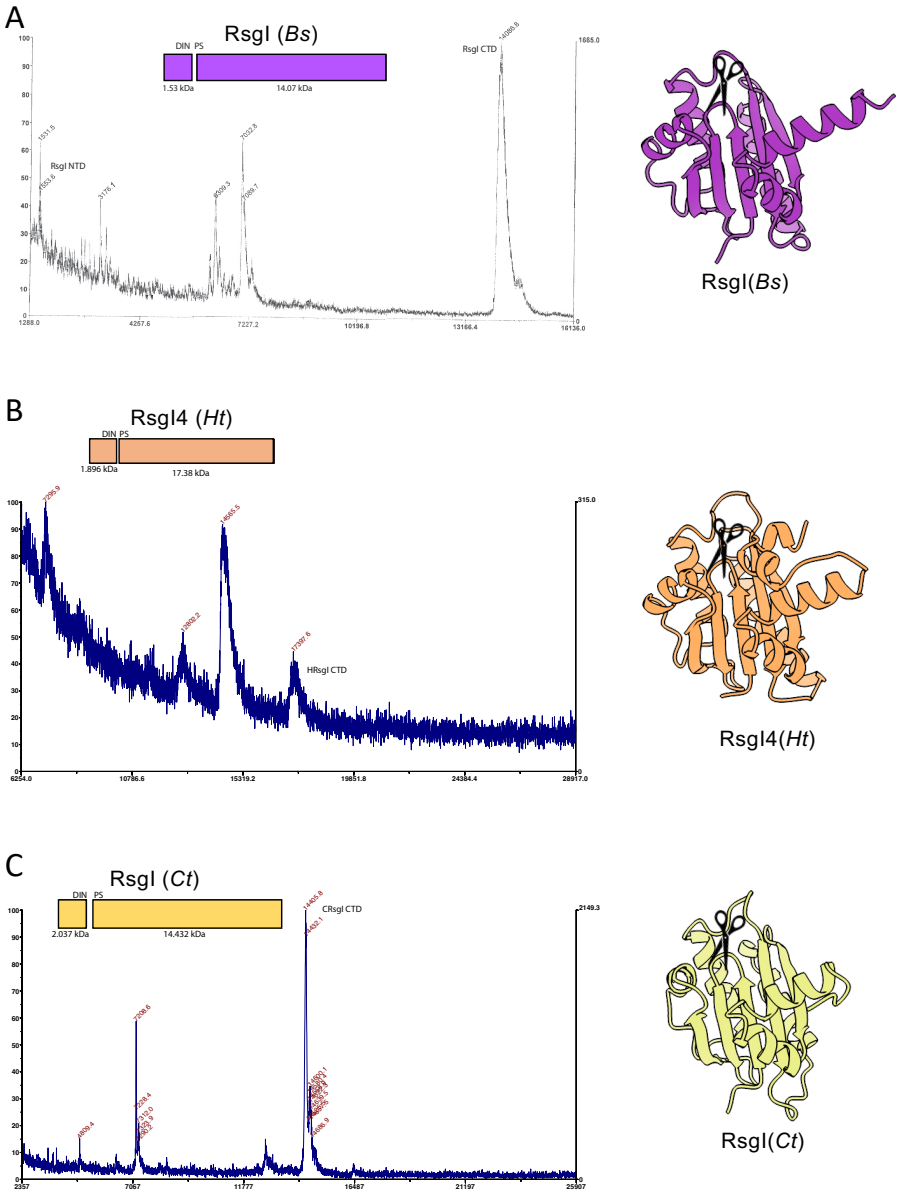

Figure S4. Intact mass spectrometry reveals a conserved cleavage site for RsgI homologs. Mass spectra of purified RsgI(SEAL) variants lacking His-SUMO tags. Protein diagrams indicating the predicted masses of the cleavage products are shown above each spectrum. AlphaFold-predicted structures and cleavage sites (scissors) are shown on the right.

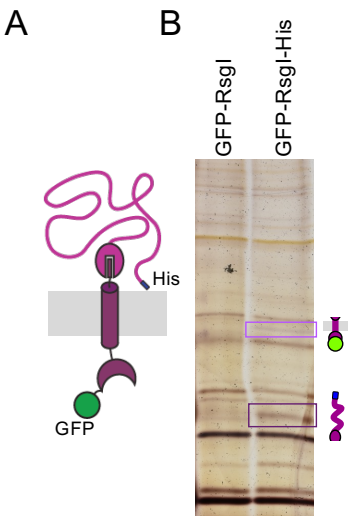

MRRGIIVEKNKKFVTLLTPDGQFLKAKNDRHSYEIGEEIMLPSETRMGRRASFF
DFFKLRPFKMGIFTMTAIMLFIFIVLPVFSNNK**AYAYMTIDIN**.PSVEMALNSD
YEVIELTPLNDEGQKVVNDIDDWEKTDFKKVIDDIITDCSEHGYVKKSK**EILIS**
TVYENTEDNTYKKAVKKQLNDVTEKYKTTYRMESLESDMQTREKAKKEGVSTGS
YIKSNEKNDNKDIKDDSSKPSGEEDQKSDENEDENTDQTDTQDSKQGDNEQLND
ADSGDQKEEKADDQIDDSDKDKKIKESDENTNTEKDGDHEQTPIQDPQDKGNEN
NGADKGQSQYHRDWNNGEQGKNRSSSRRDNASDRRNPNGYSSDNHSAKNEDSPS
APGE

Figure S5. Site-1 cleavage in vivo is consistent with the autocleavage site in vitro.
(A) Schematic of the GFP-RsgI-His6 fusion used in the assay. **(B)** Silver-stained SDS-PAGE gel of eluates from Ni^{2+}-affinity chromatography of detergent-solubilized membrane fractions from *B. subtilis* cells expressing GFP-RsgI-His6 or GFP-RsgI. The RsgI fragments (boxed in light and dark purple) were excised, digested with trypsin, and analyzed by mass spectrometry. **(C)** Sequence of RsgI with N- and C-terminal cleavage products based on the in vitro autocleavage analysis highlighted in different shades of purple. The period (.) indicates the autocleavage site identified in vitro. Sequences highlighted in yellow indicate peptides detected by MS. The two peptides in bold lack a canonical tryptic cleavage site and are therefore candidates for the site of site-1 cleavage.

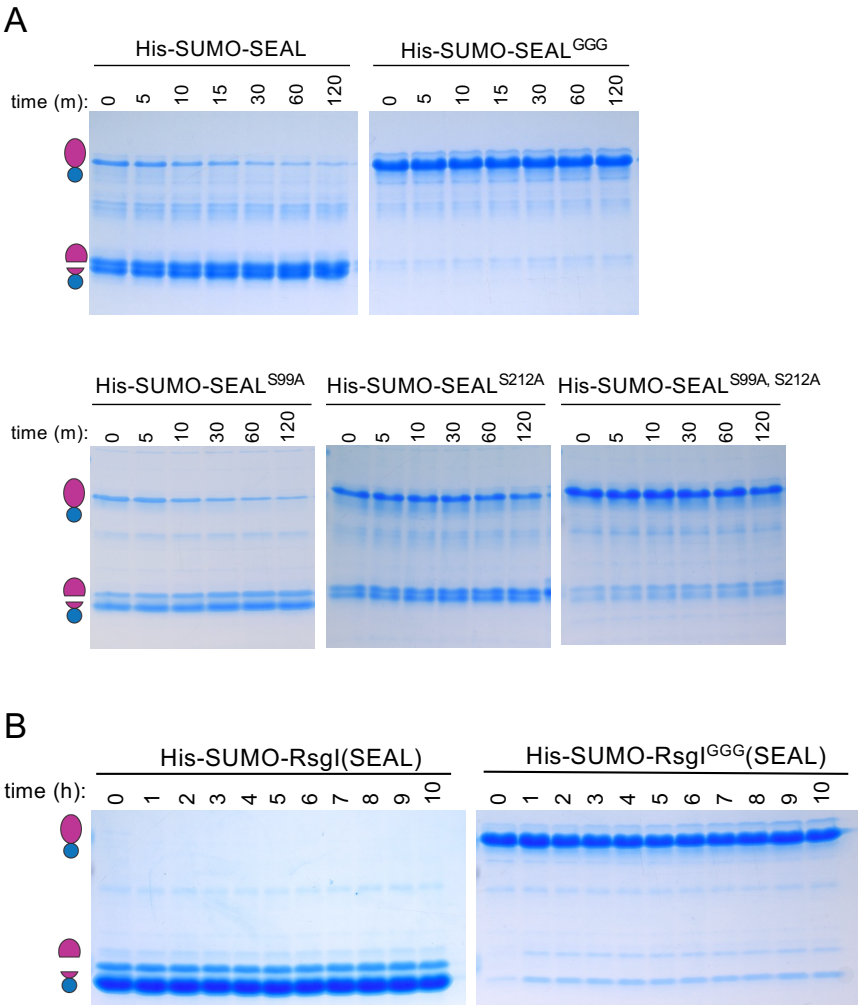

Figure S6. Point mutations in the SEAL domain fail to abolish autoproteolysis in vitro. **(A)** Commassie-stained gels of purified His-SUMO-SEAL and the indicated mutants incubated at 37 ˚C for the indicated time in minutes. All point mutants retain some autocleavage activity. **(B)** Coomassie-stained gels of purified His-SUMO-RsgI(SEAL) and the GGG variant incubated at 37 ˚C for the indicated time in hours. The SEAL^{GGG} variant undergoes modest autoproteolysis. All purifications and timecourses were performed at least two times.

A

B

Length of Chain 1 (crystal)	135
Length of Chain 2 (AlphaFold)	135
Aligned length	135
RMSD	1.08 Å
SeqID	1
TMscore (normalized by chain 1)	0.97282
Tmscore (normalized by chain 2)	0.97282

C

D

Length of Chain 1 (crystal)	135
Length of Chain 2 (MUC1 SEA)	107
Aligned length	59
RMSD	3.21
SeqID	0.102
TMscore (normalized by chain 1)	0.31465
Tmscore (normalized by chain 2)	0.37305

Figure S7. The X-ray crystal structure of SEAL^{GGG} closely resembles the AlphaFold2-predicted model and is structurally similar to MUC1's SEA domain. (A) Structural alignment of the AlphaFold-predicted (dark purple) and experimentally determined (light purple) SEAL^{GGG} domains by TM-align. **(B)** Metrics describing the structural alignment. **(C)** Structural alignment of the x-ray crystal structure of SEAL^{GGG} and MUC1's SEA (green) domains. **(D)** Metrics describing the structural alignment.

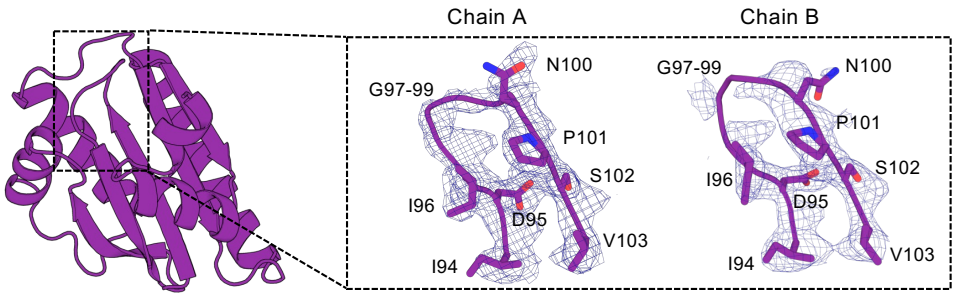

Figure S8. The glycine loop in the SEAL^{GGG} domain is highly flexible. Overview cartoon diagram of the SEAL structure with a detailed view of the "GGG loop" for both chains in the crystal asymmetric unit. Mesh represents the 2Fo-Fc map contoured at 1.0σ. The full loop on chain B is not resolved.

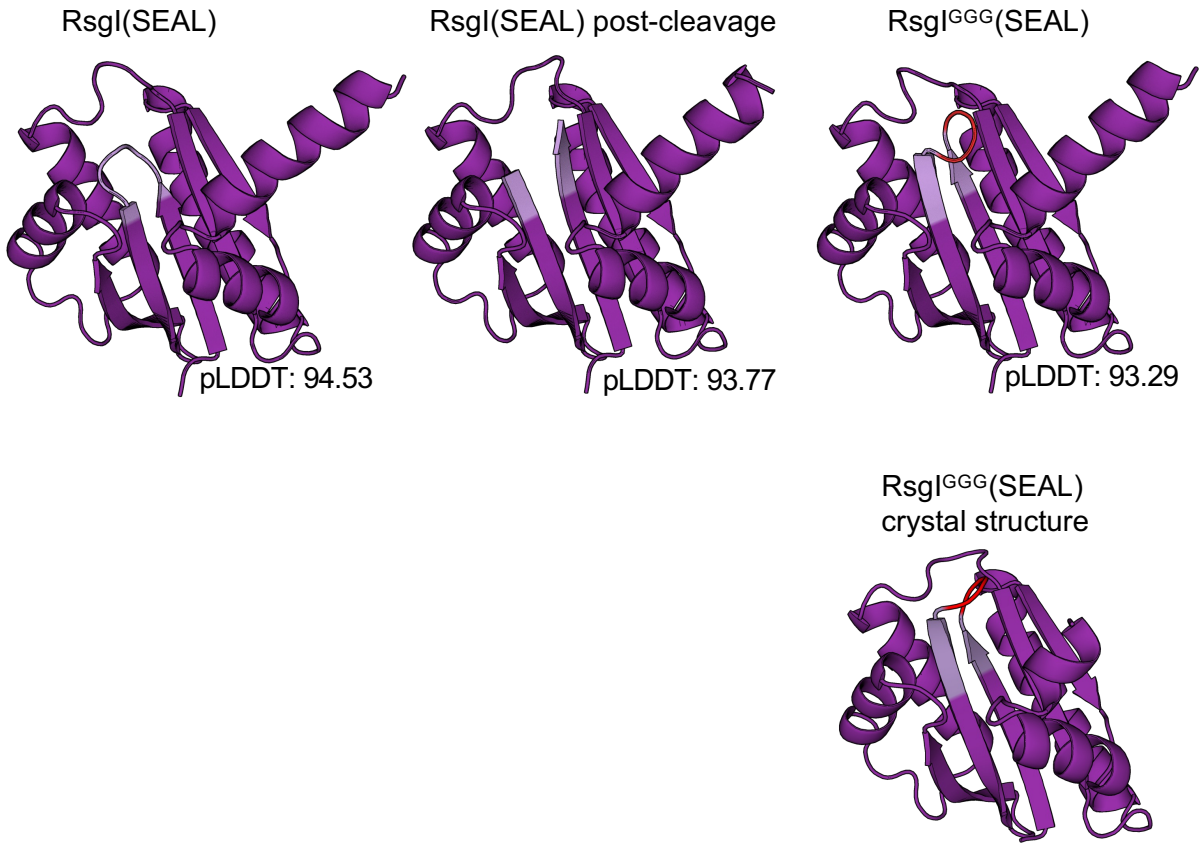

Figure S9. Alphafold2 predicts similar structures for autocleaved RsgI and RsgI^{GGG}. AlphaFold2 predictions of uncleaved (left) and GGG variant (right) of RsgI's SEAL domain compared to the AlphaFold-multimer prediction of the two cleaved fragments (middle). The conserved beta hairpin loop (DINPS) is colored in light purple and the inserted glycines colored in red. The cleaved SEAL domain and the GGG variant are both predicted to have extended ß-strands. This extension is confirmed in the SEAL^{GGG} crystal structure (bottom right).

Figure S10
Brogan *et al.*

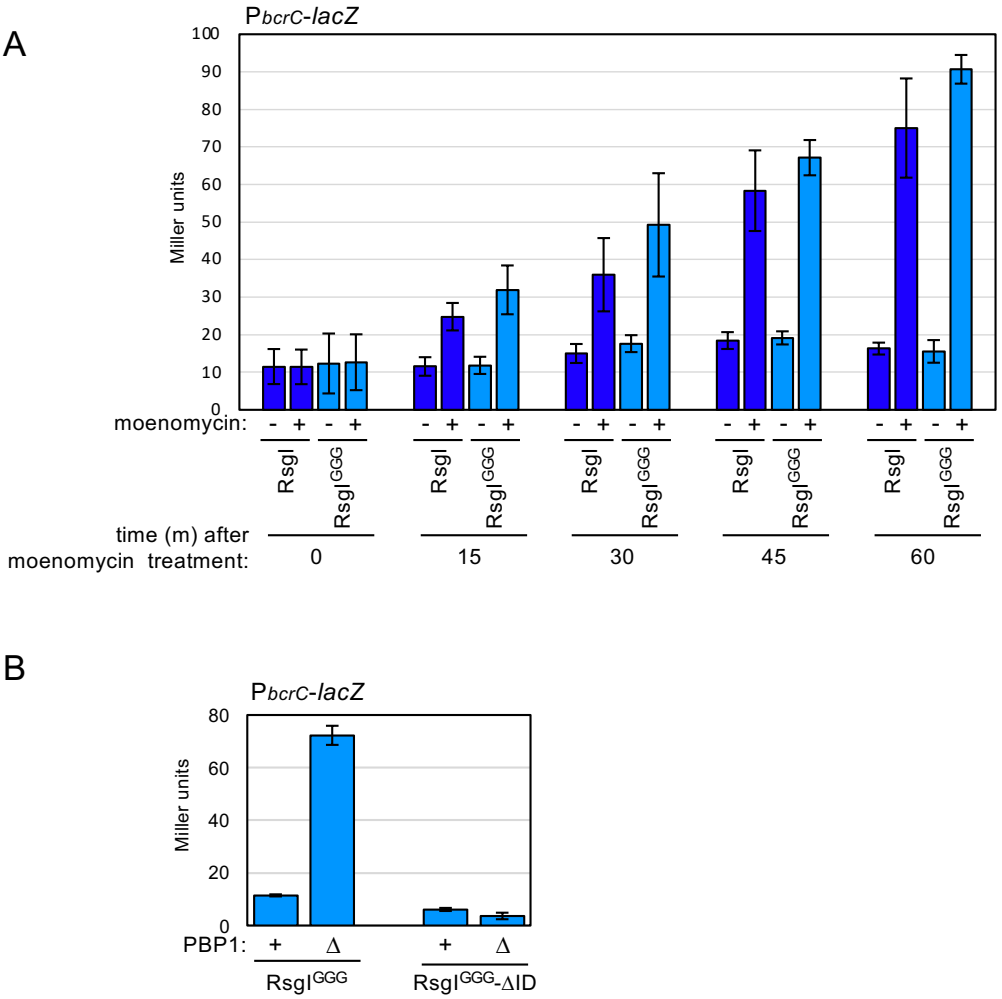

Figure S10. RsgI^{GGG} responds to cell wall defects in a manner that depends on its intrinsically disordered region. (A) Bar graph showing ß-galactosidase activity of a SigI-responsive (P_{bcrC}) reporter before and after addition of moenomycin. Strains harboring untagged RsgI and RsgI^{GGG} respond similarly over a 60 min time course. **(B)** Bar graph showing beta-galactosidase activity of cells expressing RsgI^{GGG} or RsgI^{GGG}ΔID in the presence and absence of PBP1. If RsgI^{GGG} lacks its intrinsically disordered region (ΔID), the cells are unable to respond to cell wall defects. All ß-galactosidase assays were performed in biological triplicate and error bars indicate standard error among them.

Figure S11
Brogan *et al.*

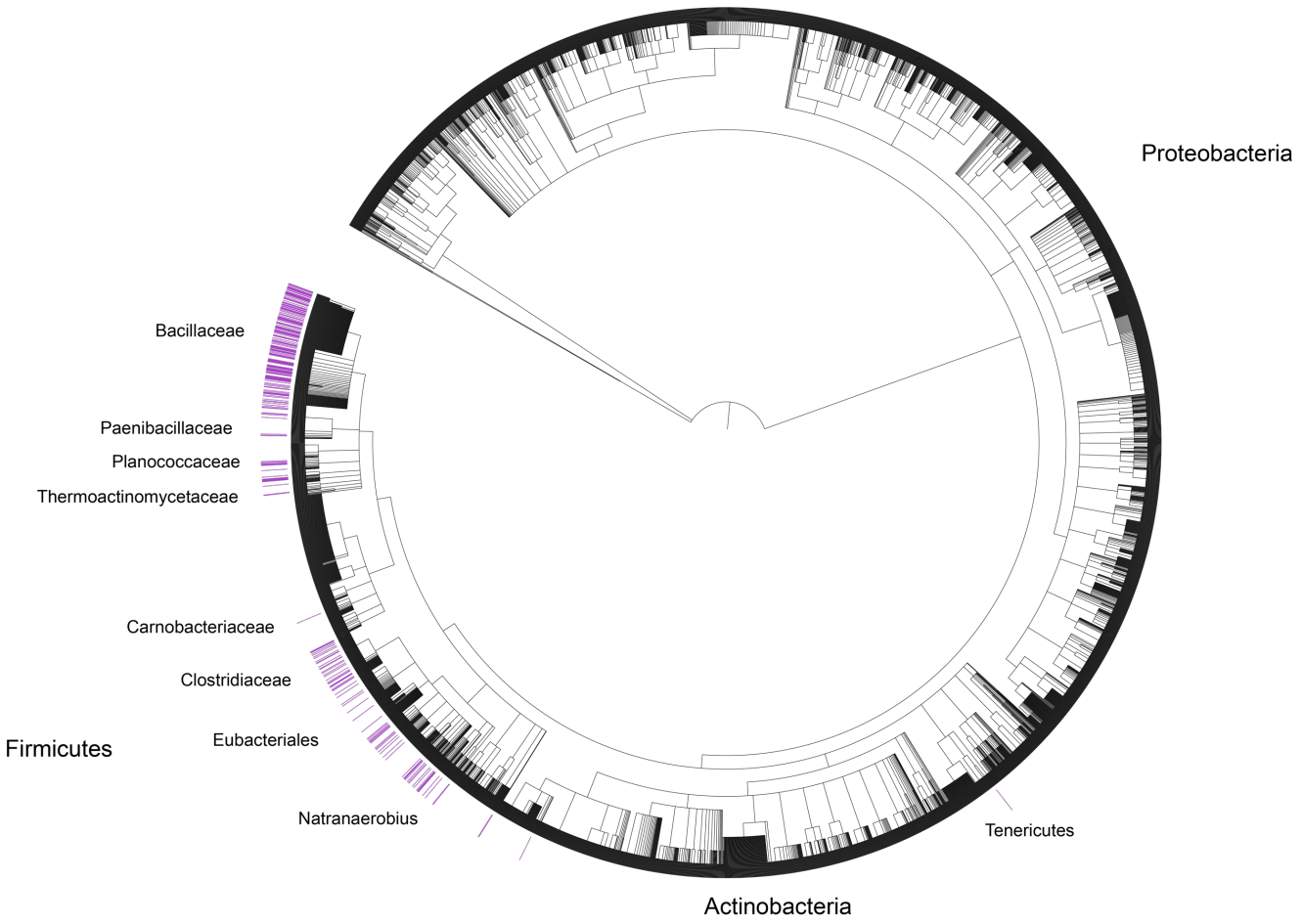

Figure S11. SEAL domains are broadly conserved among Firmicutes. Phylogenetic tree showing distribution of SEAL domains throughout 5767 bacterial taxa. The amino acid sequence of *B. subtilis* RsgI's SEAL domain was used to query the Refseq database and the resulting species containing SEAL homologs are annotated in purple.

Figure S12
Brogan *et al.*

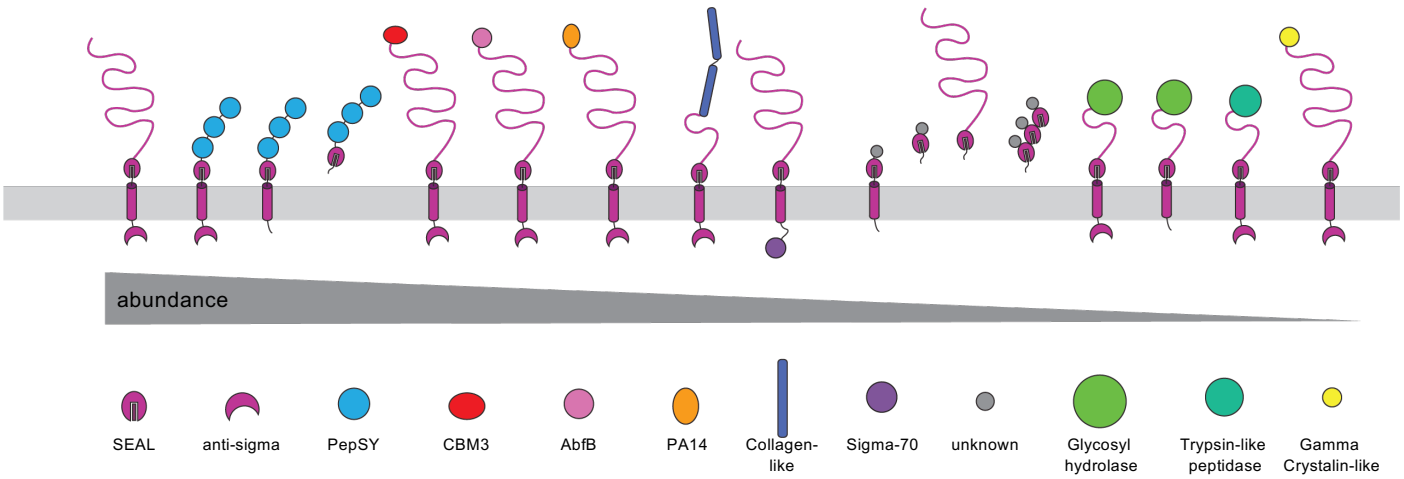

Figure S12. SEAL domains are found in proteins with diverse domain architectures. Schematics of proteins with SEAL domains found across Firmicutes. The amino acid sequence of *B. subtilis* RsgI's SEAL domain was used to search the Refseq select protein database for sequence homologs. The resulting protein FASTA files were annotated for known Pfam domains using PfamScan. The protein architectures were reconstructed by binning the identified Pfam domains by protein accession number in the order identified. The protein families are displayed from most to least abundant. All SEAL-containing domains are predicted to be extracytoplasmic and either fused to a TM segment or a signal peptide.

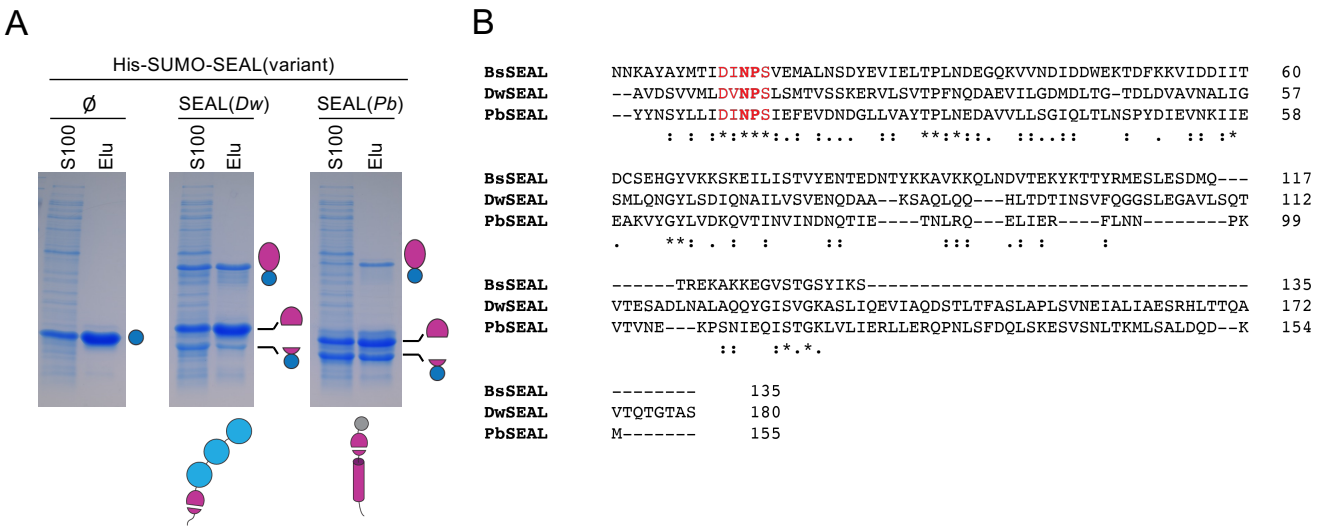

Figure S13. Autoproteolysis is a conserved feature of SEAL domains. **(A)** Coomassie-stained gels of His-SUMO(SEAL) homologs from *D. welbionis* (*Dw*) (EIO64_09220) and *P. brassicae* (*Pb*) (BN85316100) expressed and purified from *E. coli*. His-SUMO lacking a SEAL domain (ø) was included as a control. Schematics of full-length proteins are shown below the gels. The *B. welbionis* protein has a predicted signal peptide, a SEAL domain, and three putative PepSY domains. The *P. brassicae* protein has a TM segment, a SEAL domain, and a domain of unknown function. The domain is unannotated by Pfam but is conserved across homologs as a predicted six α-helical bundle with no characteristic sequence or structural homology. The *P. brassicae* protein lacks a sigma factor binding domain. **(B)** Multiple sequence alignment of *B. subtilis*, *D. welbionis*, and *P. brassicae* SEAL domains. The conserved beta-hairpin that is the site of autocleavage is highlighted in red, and the cleavage site is in bold.

Supplemental Tables

Table S1. Hits from the DALI server search with Alphafold predicted *Bacillus subtilis* SEAL

	Description	***Organism***	***Chain***	***Z score***	***RMSD***	***Length***	***#Resi***	***% ID***
1	Protein N-terminal asparagine amidohydrolase	*Homo sapiens*	6a0e-A	6.1	2.7	85	305	5
2	YlmD (cysteine hydrolase)	*Geobacillus stearothermophilus*	Lt8h-A	5.6	2.7	74	272	9
3	APOBEC3H (mRNA editing enzyme)	*Macaca nemestrina*	5w3v-A	5.6	3.2	83	186	5
4	Deep network hallucinated protein	De novo synthetic construct	7m0q-B	5.5	2.8	79	97	6
5	APOBEC3H (mRNA editing enzyme)	*Macaca mulatta*	6p40-A	5.5	6	91	364	3
6	TOP7 surface mutant	De novo synthetic	7fao-A	5.5	3	76	96	13
7	De novo designed protein	De novo synthetic	2mra-A	5.4	3	84	117	15
8	NTPDase 2 (nucleoside triphosphate hydrolase)	*Rattus norvetigcus*	4br5-A	5.4	3.7	110	422	4
9	De novo designed beta sheet	De novo synthetic	4kyz-A	5.3	5	82	167	11
10	VASH2/SVBP (tubulin-tyrosine carboxypeptidase)	*Homo sapiens*	6jze-A	5.3	3.9	76	254	7

Table S2. Summary of data collection, phasing and refinement statistics

	RsgI (8T9N)
Data collection	
Space group	P 1 2_1 1
Cell dimensions	
a, *b*, *c* (Å)	38.175, 63.889, 59.935
α, β, γ (°)	90.0, 92.6, 90.0
Resolution (Å)	38.13–1.90 (1.94–1.90)
R_{pim}	3.8 (87.9)
$I / \sigma(I)$	10.1 (1.0)
Completeness (%)	98.6 (97.9)
Redundancy	3.7 (3.5)
Refinement	
Resolution (Å)	38.13–1.90
No. reflections	
Total	82070
Unique	22424
Free	1994
R_{work} / R_{free}	23.03 / 27.48
No. atoms	
Protein	1983
Ligand / ion	–
Water	80
B-factors	
Protein	62.65
Ligand / ion	–
Water	54.73
R.m.s. deviations	
Bond lengths (Å)	0.004
Bond angles (°)	0.688
Ramachandran (favoured/allowed)	97.92 / 0.88
Rotamer Outliers	0.88
MolProbity Score	1.60

*Dataset was collected from individual crystals.
**Values in parentheses are for the highest resolution

Table S3. SEAL PfamScan results

Pfam	Name	Count
PF12791	Anti-sigma factor N-terminus	2914
PF03413	Peptidase propeptide and YpeB (PepSY) domain	229
PF00942	Cellulose binding domain (CBM3)	11
PF05270	Alpha-L-arabinofuranosidase B (AbfB) domain	10
PF07691	PA14 Domain	7
PF01391	Collagen triple helix repeat	6
PF13365	Trypsin-like peptidase domain	5
PF04542	Sigma-70 region 2	3
PF00030	beta/gamma crystallin-like	1
PF00331	Glycosyl hydrolase family 10	1

Table S4. Strains used in this study

Strain	Background	Genotype	Reference	Figure
BAB325	*B.subtilis PY79*	*yvbJ::PxylA-gfp-RsgI-His (erm) ΔrsgI::spc*	This Study	5
BAB331	*B.subtilis PY79*	*yvbJ::PxylA-gfp-RsgI-DI-GGG-NPS-His (erm) ΔrsgI::spc*	This Study	5, 6
BAB332	*B.subtilis PY79*	*yvbJ::PxylA-gfp-RsgI-His (erm) ΔrsgI::spc ΔponA::kan*	This Study	5
BAB338	*B.subtilis PY79*	*yvbJ::PxylA-gfp-RsgI-DI-GGG-NPS-His (erm) ΔrsgI::spc ΔponA::kan*	This Study	5, 6
BAB19	*B.subtilis PY79*	*sacA::Pveg-gfp (Phleo) yhdG::PbcrC-optRBS-lacZ (cat) Δ(sigI-rsgI)::spc amyE::sigI-rsgI (kan)*	This Study	5, S10
BAB29	*B.subtilis PY79*	*sacA::Pveg-gfp (Phleo) yhdG::PbcrC-optRBS-lacZ (cat) Δ(sigI-rsgI)::spc amyE::sigI-rsgI (kan) ΔponA::erm*	This Study	5, S10
BAB321	*B.subtilis PY79*	*sacA::Pveg-gfp (Phleo) yhdG::PbcrC-optRBS-lacZ (cat) Δ(sigI-rsgI)::spc amyE::sigI-rsgI-DI-GGG-NPS (kan)*	This Study	5, S10
BAB323	*B.subtilis PY79*	*sacA::Pveg-gfp (Phleo) yhdG::PbcrC-optRBS-lacZ (cat) Δ(sigI-rsgI)::spc amyE::sigI-rsgI-DI-GGG-NPS (kan) ΔponA::erm*	This Study	5, S10
BAB443	*B.subtilis PY79*	*sacA::Pveg-gfp (Phleo) yhdG::PbcrC-optRBS-lacZ (cat) Δ(sigI-rsgI)::spc amyE::sigI-rsgI-DI-GGG-NPS-ΔID (kan)*	This Study	S10
BAB447	*B.subtilis PY79*	*sacA::Pveg-gfp (Phleo) yhdG::PbcrC-optRBS-lacZ (cat) Δ(sigI-rsgI)::spc amyE::sigI-rsgI-DI-GGG-NPS-ΔID (kan) ΔponA::erm*	This Study	S10
BAB450	*B.subtilis PY79*	*yvbJ::PxylA-gfp-RsgI-DI-GGG-NPS-ΔID-His (erm) ΔrsgI::spc*	This Study	6
BAB453	*B.subtilis PY79*	*yvbJ::PxylA-gfp-RsgI-DI-GGG-NPS-ΔID-His (erm) ΔrsgI::spc ΔponA::kan*	This Study	6
BAB339	*B.subtilis PY79*	*yvbJ::PxylA-gfp-RsgI-His (erm) ΔrsgI::spc ΔrasP::tet*	This Study	6
BAB345	*B.subtilis PY79*	*yvbJ::PxylA-gfp-RsgI-DI-GGG-NPS-His (erm) ΔrsgI::spc ΔrasP::tet*	This Study	6

Table S5. Plasmids used in this study

Plasmid	Description	Reference
pCH26	His-SUMO-*Ct*RsgI(JMD) (amp)	This Study
pCH27	His-SUMO-*Ht*RsgI4(JMD) (amp)	This Study
pCH29	His-SUMO-*Bs*RsgI(JMD) (amp)	This Study
pYB72	amyE::sigI-rsgI-S481UTR (kan)(amp)	Brunet et al.
pYB200	yvbJ::PxylA-gfp-His6 (erm)(amp)	Brunet et al.
pYB202	amyE::sigI-rsgIΔID-S481UTR (kan)(amp)	Brunet et al.
pYB225	amyE::sigI-NheI-S481UTR (kan)(amp)	Brunet et al.
pYB240	yvbJ::PxylA-gfp-rsgIΔID-His6 (erm)(amp)	Brunet et al.
pAB61	yvbJ::PxylA-gfp-rsgI-His6 (erm)(amp)	This Study
pAB78	yvbJ::PxylA-gfp-rsgI-DI-GGG-NPS-His6 (erm)(amp)	This Study
pAB79	His-SUMO-RsgI(JMD)-DI-GGG-NPS (amp)	This Study
pAB87	P_{T7}-GFP-RsgI(JMD) (amp)	This Study
pAB90	amyE::sigI-rsgI-DI-GGG-NPS-S481UTR (kan)(amp)	This Study
pAB93	His-SUMO-*Ht*RsgI2(JMD) (amp)	This Study
pAB101	P_{T7}-GFP-RsgI(JMD)-DI-GGG-NPS (amp)	This Study
pAB129	amyE::sigI-rsgI-DI-GGG-NPS-ΔID-S481UTR (kan)(amp)	This Study
pAB130	yvbJ::PxylA-gfp-rsgI-DI-GGG-NPS-ΔID-His6 (erm)(amp)	This Study
pAB188	His-SUMO-RsgI-GGG(JMD)-A88-S219 (amp)	This Study
pAB214	His-SUMO-SEAL(*Dwelbionis*) (amp)	This Study
pAB216	His-SUMO-SEAL(*Pbrassicae*) (amp)	This Study

Table S6. Oligonucleotides used in this study

Oligo	Sequence
oAB35	TTATTTAAAAGATTATCTTAAAGGGGTGCTGCACTCATGAGAAGAGGGATTATAGTAGAG
oAB36	AATTAAATGGCACAACTAAATAAATTCAGGTCTTTATTCGCCG
oAB112	tatacaaaGGATCAGGCCTCGAGagaagagggattatagtagagaaaaataaaaaattcg
oAB113	GAGGGTTGCCAGAGTTAAATTAATGATGGTGATGATGATGttcgccgggggcactcg
oAB117	TATTACTCGAGGAGCTCGGATTATGATTTGATGTAGCTGCCTGTAGCGACGCCTTCTTTC
oAB128	cttggattGCCGCCGCCgatatcgattgtcatatacgcataggcc
oAB129	cgatatcGGCGGCGGCaatccaagcgtcgaaatggcg
oAB141	GTTTAACTTTAAGAAGGAGATATACATatgagtaaaggagaagaacttttcactgg
oAB142	TACTCGAGAATTCCCGGGATCCTTATGATTTGATGTAGCTGCCTGTTGAG
oAB143	actatacaaaGGATCAGGCCTCGAGAATAATAAGGCCTATGCGTATATGACAATCG
oAB144	GTCATATACGCATAGGCCTTATTATTCTCGAGGCCTGATCCtttgtatag
oAB154	GGCTCACAGAGAACAGATTGGTGGAGTCTCCATATCCCAAGAGTACGC
oAB155	AGCTTATTACTCGAGGAGCTCGGATTAAAACTTACCGATATTTACCTTACCCAAAATTTC
oAB356	GAGGCTCACAGAGAACAGATTGGTGGAGCCTATGCGTATATGACAATCGATATCAATCC
oAB410	GGCTCACAGAGAACAGATTGGTGG
oAB411	CAAGCTTATTACTCGAGGAGCTCGG
oAB412	GCTCACAGAGAACAGATTGGTGGATACTACAACTCATATTTACTGATCGACATTAACCCG
oAB413	AAGCTTATTACTCGAGGAGCTCGGATTACATTTTGTCTTGATCCAAGGCGCTTAAC
oCH53	GAGGCTCACAGAGAACAGATTGGTGGAAATAATAAGGCCTATGCGTATATGACAATCG
oCH54	CGACAAGCTTATTACTCGAGGAGCTCGGATGATTTGATGTAGCTGCCTGTTGAGACG
oCH63	GGTGGTGCTCGACAAGCTTATTACTCGAGGAGCTCGGATTAttcttgcttgagtttctc
oCH65	GTGGTGCTCGACAAGCTTATTACTCGAGGAGCTCGGATTAattttccaatgtttctgac
oCH66	CGATATTATTGAGGCTCACAGAGAACAGATTGGTGGAggcttgcataattttaatg
oCH69	GGTGGTGCTCGACAAGCTTATTACTCGAGGAGCTCGGATTATGATTTGATGTAGCTGCC
oYB425	CAGGTCTTTAgctagcTTCGCCATTGTCATTCTTTTCATTTGATTTGATGTAGC
oYB507	TTAATGATGGTGATGATGATGTTCGCCATTGTCATTCTTTTCATTTGATTTGATGTAGC

Table S7. Gene blocks used in this study

Gblock	Sequence
*Pb*SEAL	TACTACAACTCATATTTACTGATCGACATTAACCCGTCTATAGAGTTCGAGGTTGATAATGATG GTCTGTTGGTTGCGTACACACCTCTCAACGAGGACGCCGTTGTCTTACTTAGTGGTATTCAGCT TACTCTTAACTCTCCTTACGACATTGAAGTCAATAAAATTATCGAGGAGGCAAAGGTTTATGG GTATCTGGTCGACAAACAGGTTACCATTAACGTTATCAATGATAACCAGACTATCGAAACCAA CCTGCGCCAGGAGCTTATAGAGCGTTTCCTCAATAACCCTAAAGTTACAGTGAACGAAAAGCC TTCAAACATTGAGCAGATCAGCACAGGCAAACTCGTCCTCATTGAGCGGCTGCTTGAACGCCA GCCGAACTTGTCCTTCGACCAATTAAGCAAAGAGTCCGTCTCAAACTTAACAAAAATGTTAAG CGCCTTGGATCAAGACAAAATG
*Dw*SEAL	GGCTCACAGAGAACAGATTGGTGGAGCAGTCGATTCCGTAGTAATGTTGGACGTAAATCCGA GTTTAAGTATGACTGTTTCCAGCAAAGAGCGTGTCCTTTCCGTGACCCCATTCAATCAGGATGC CGAGGTCATCCTGGGCGATATGGACCTCACGGGCACTGATTTAGATGTCGCGGTCAATGCCCT CATTGGTAGTATGCTGCAAAATGGGTATTTATCAGATATTCAGAATGCAATACTGGTCAGCGT GGAGAATCAAGATGCGGCAAAAAGCGCACAACTCCAACAGCATTTGACGGACACTATTAACT CCGTATTCCAAGGTGGATCTCTCGAAGGTGCGGTGTTAAGCCAAACGGTAACAGAGTCAGCA GACCTGAATGCGCTCGCGCAGCAGTACGGAATTAGCGTGGGCAAAGCTAGTTTGATACAGGA AGTTATCGCCCAAGACTCTACTCTTACGTTTGCAAGTTTGGCCCCATTAAGTGTAAATGAGATT GCTCTTATTGCTGAGAGCCGCCACCTCACGACTCAGGCTGTGACGCAGACAGGCACTGCCTCT TAATCCGAGCTCCTCGAGTAATAAGCTTG

Uncropped immunoblots and SDS-PAGE gels.

Figure 2A.

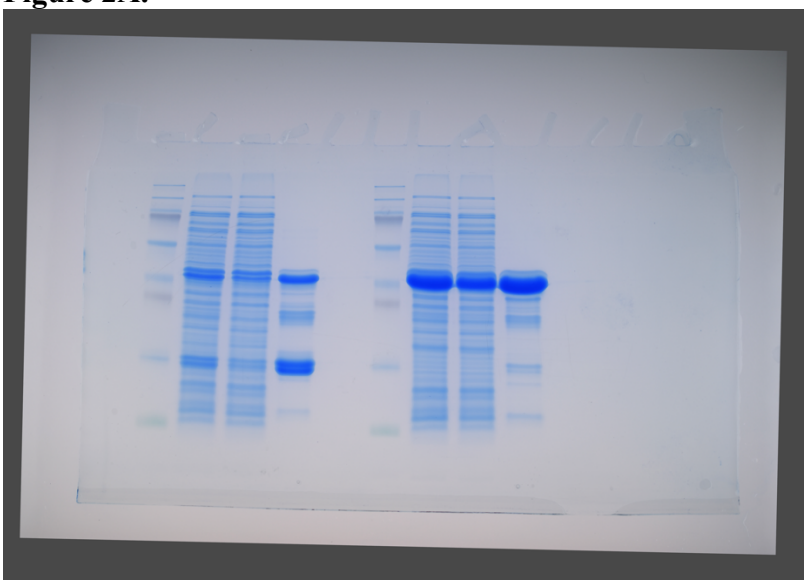

Figure 2B.

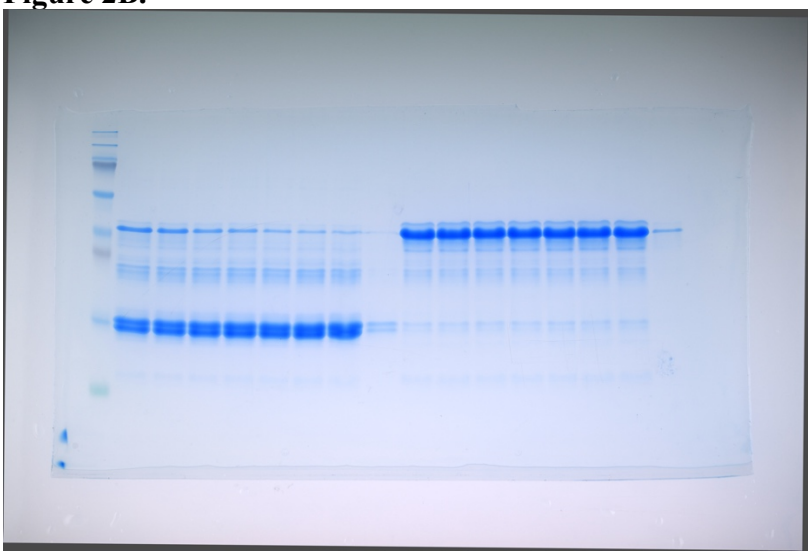

Figure 2C.

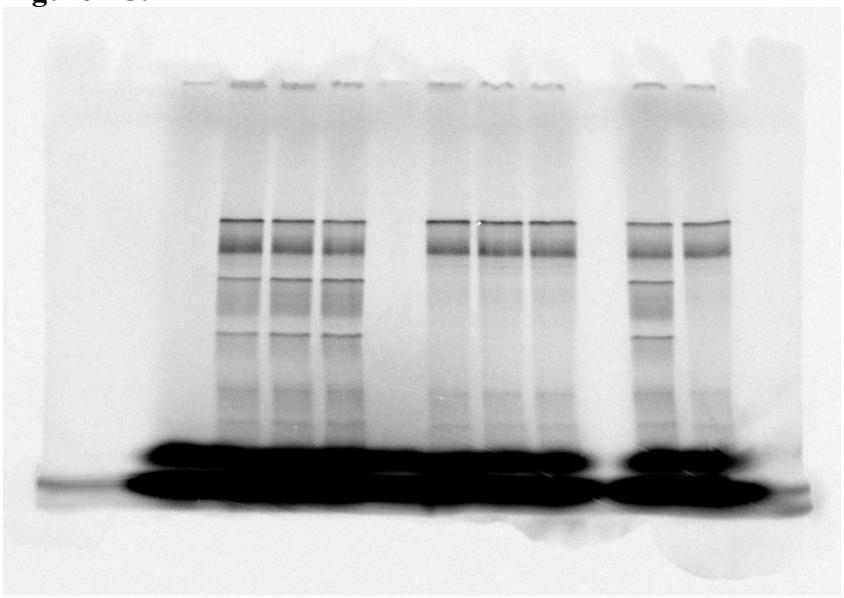

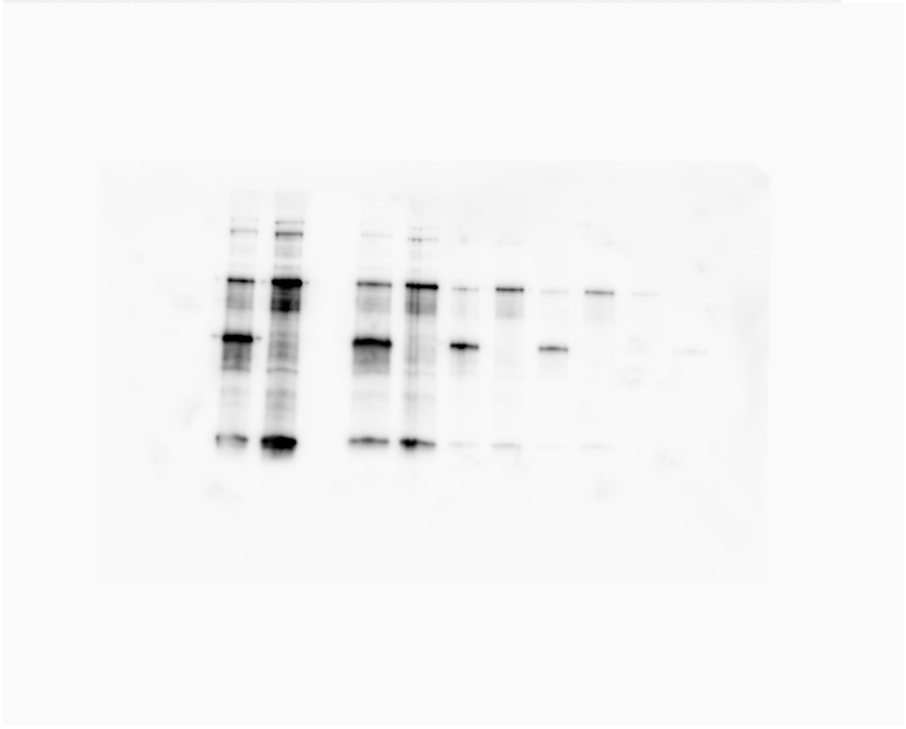

Figure 3B.

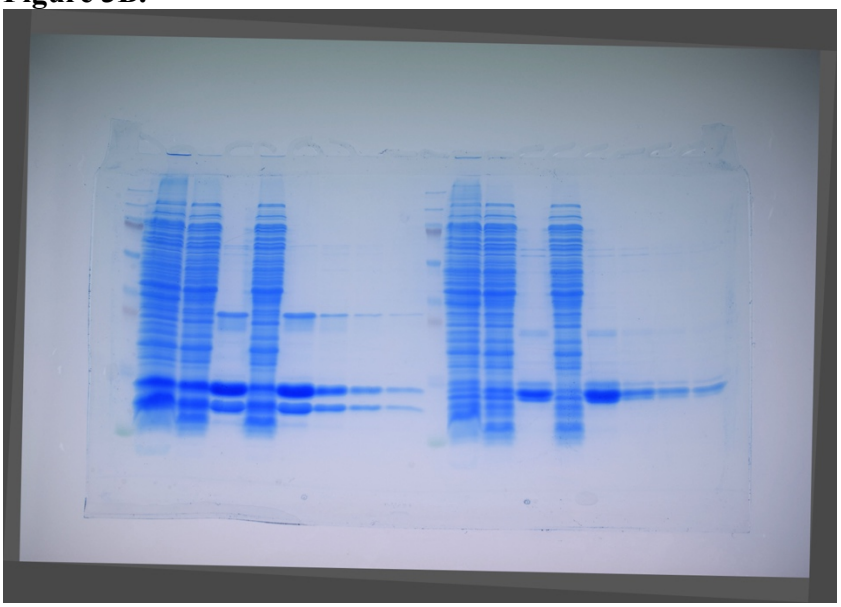

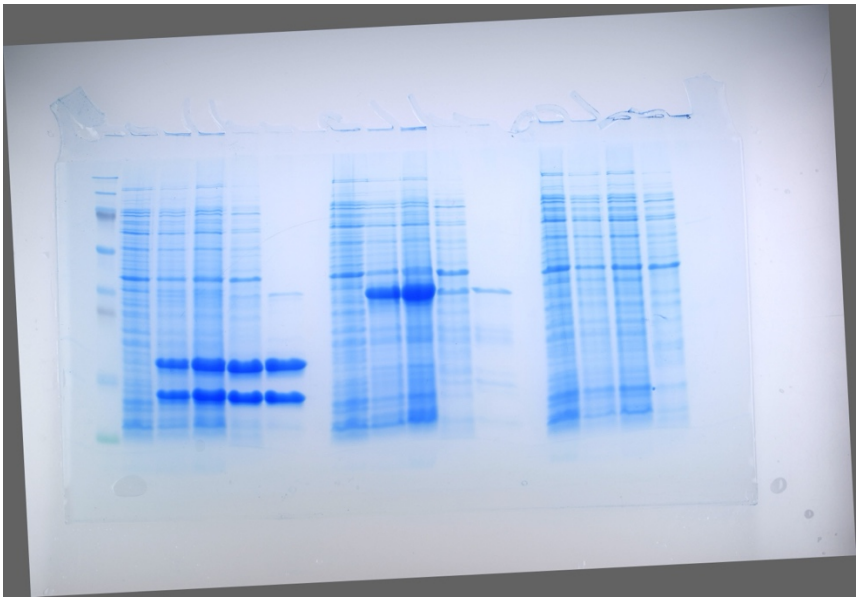

Figure 3C.

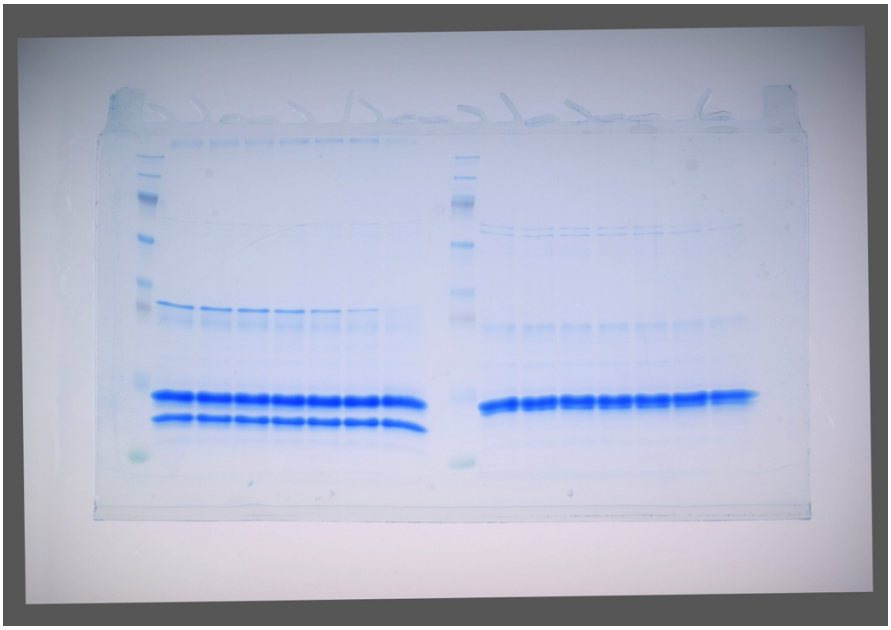

Figure 3D.

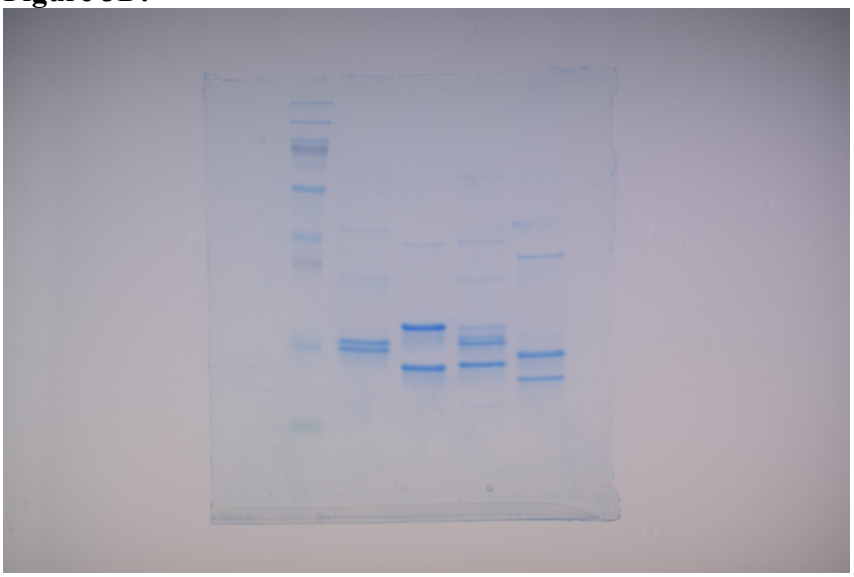

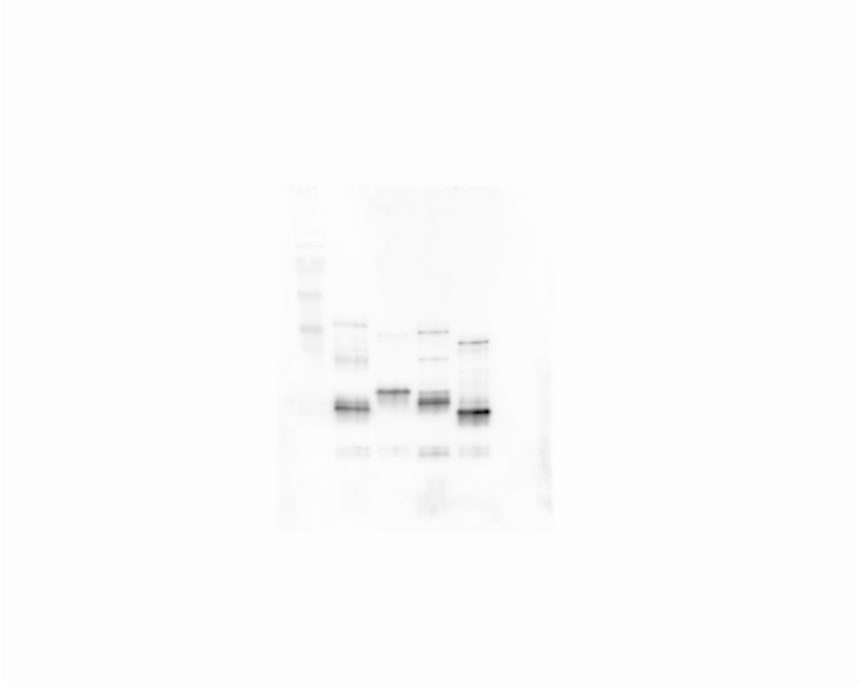

Figure 5A.

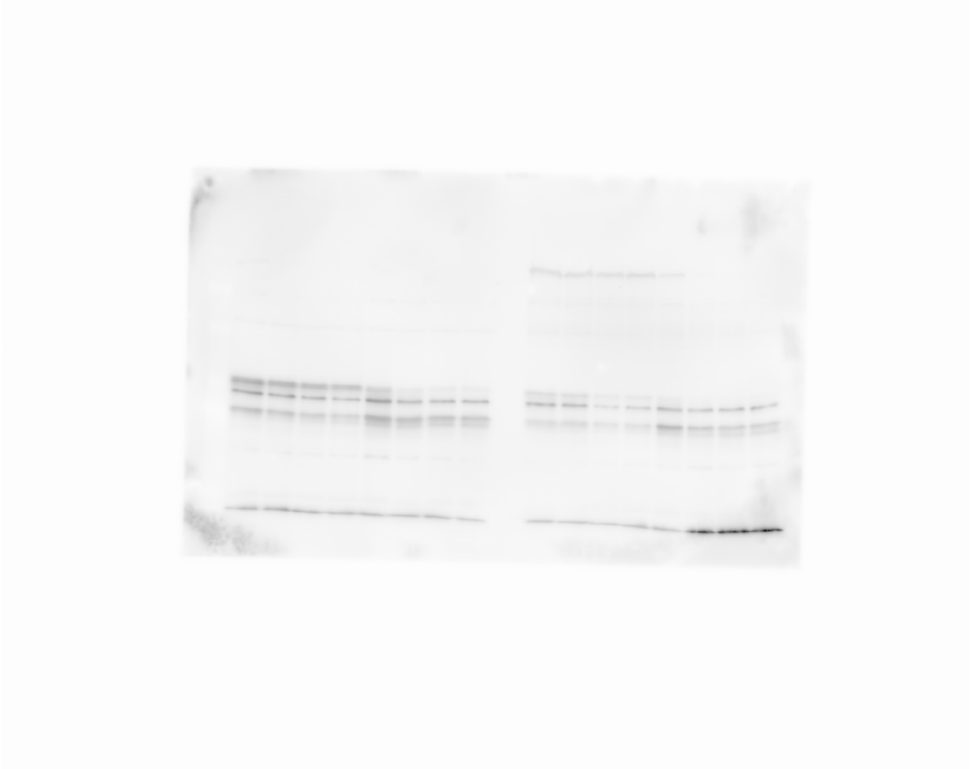

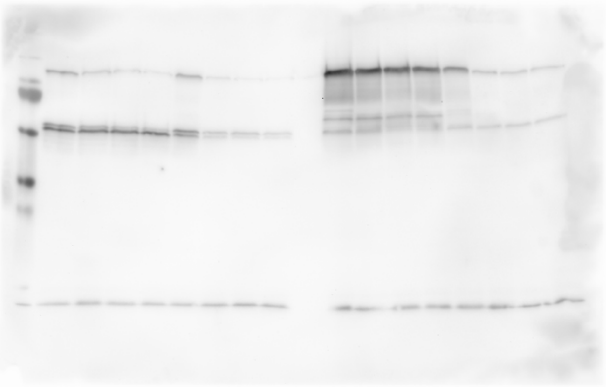

Figure 6B.

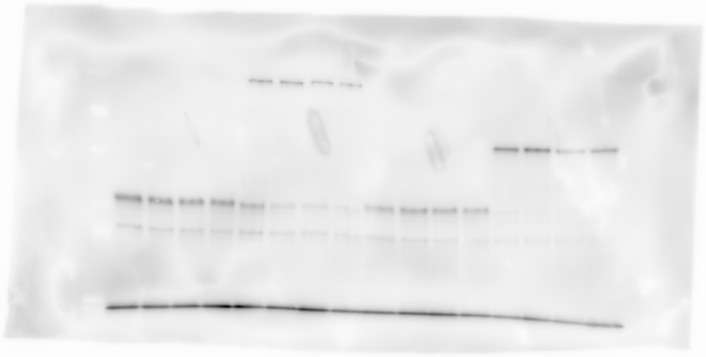

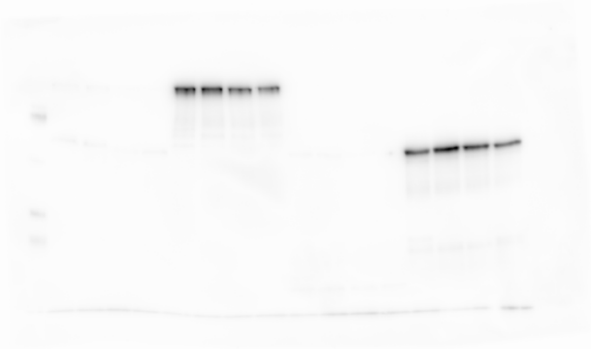

Figure 6C.

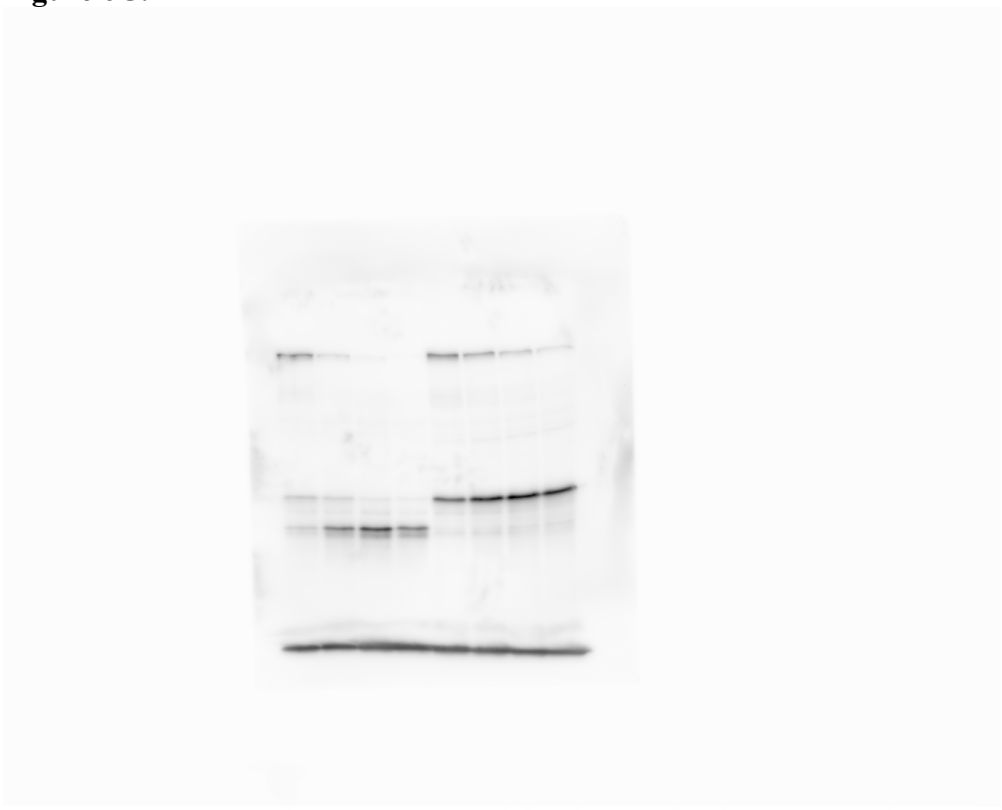

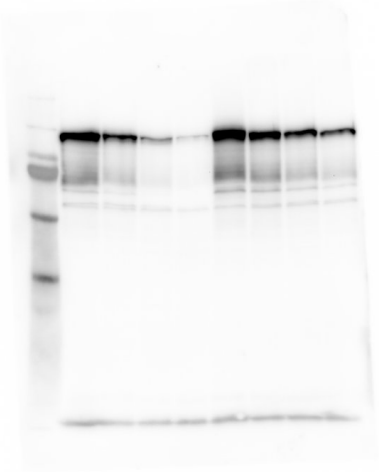

Figure S6.

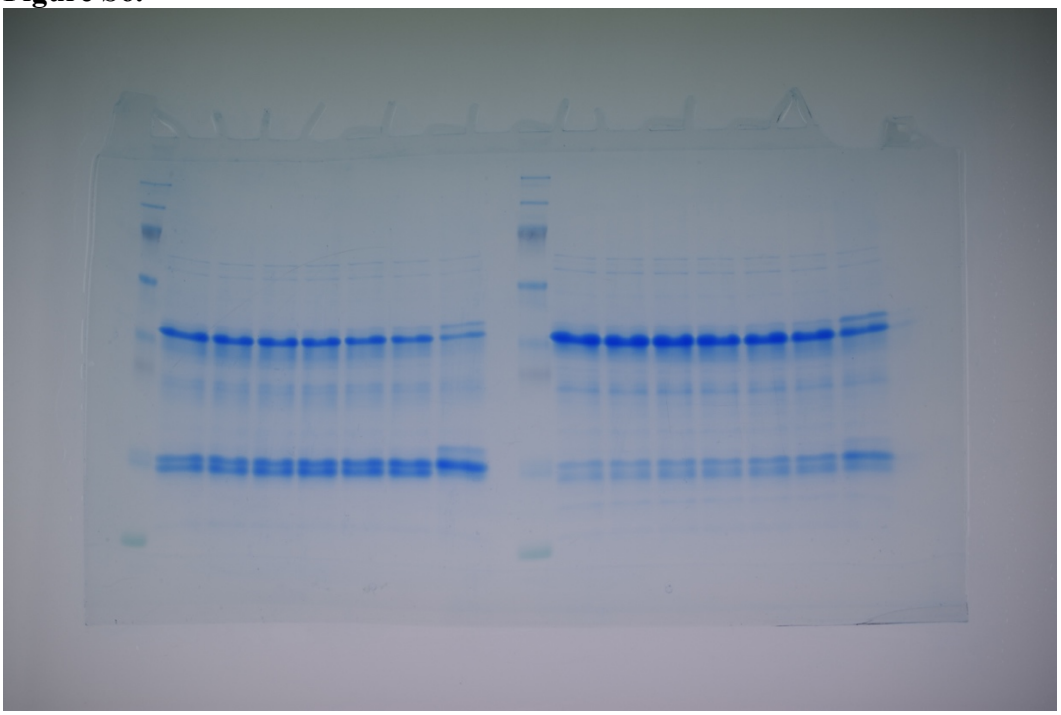

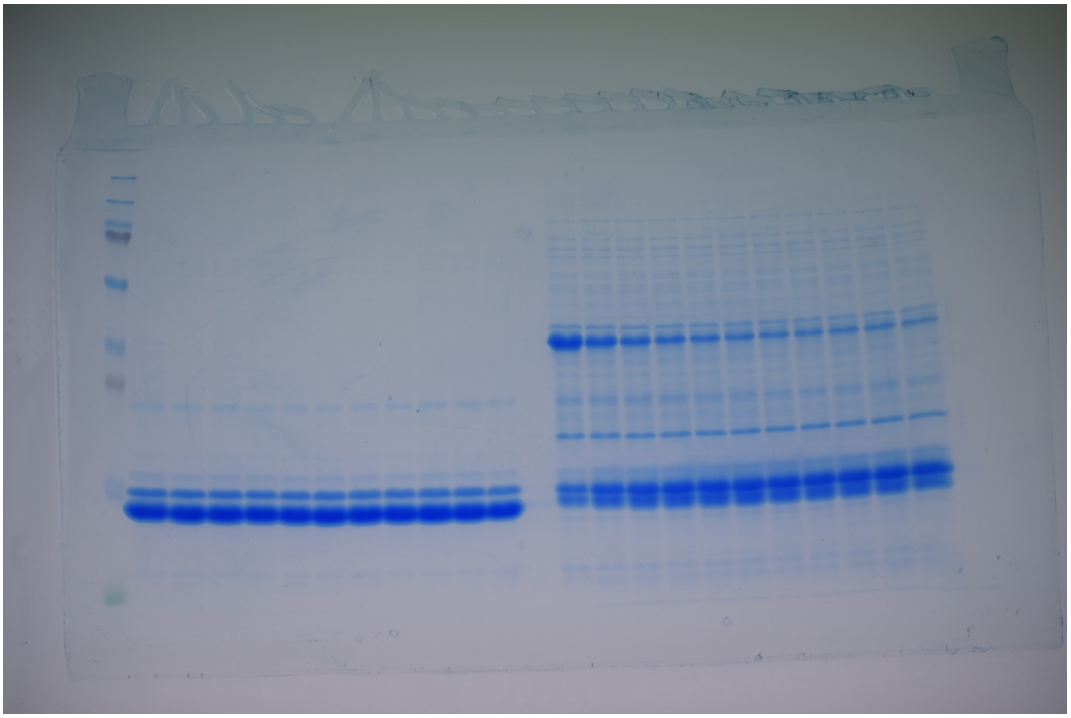

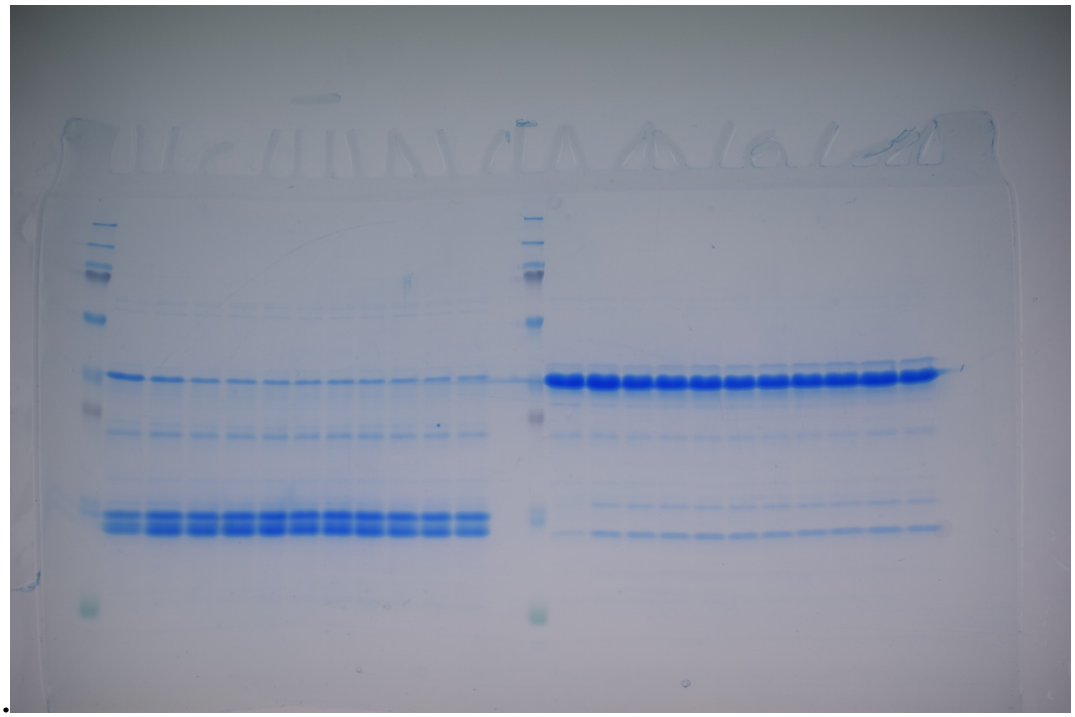

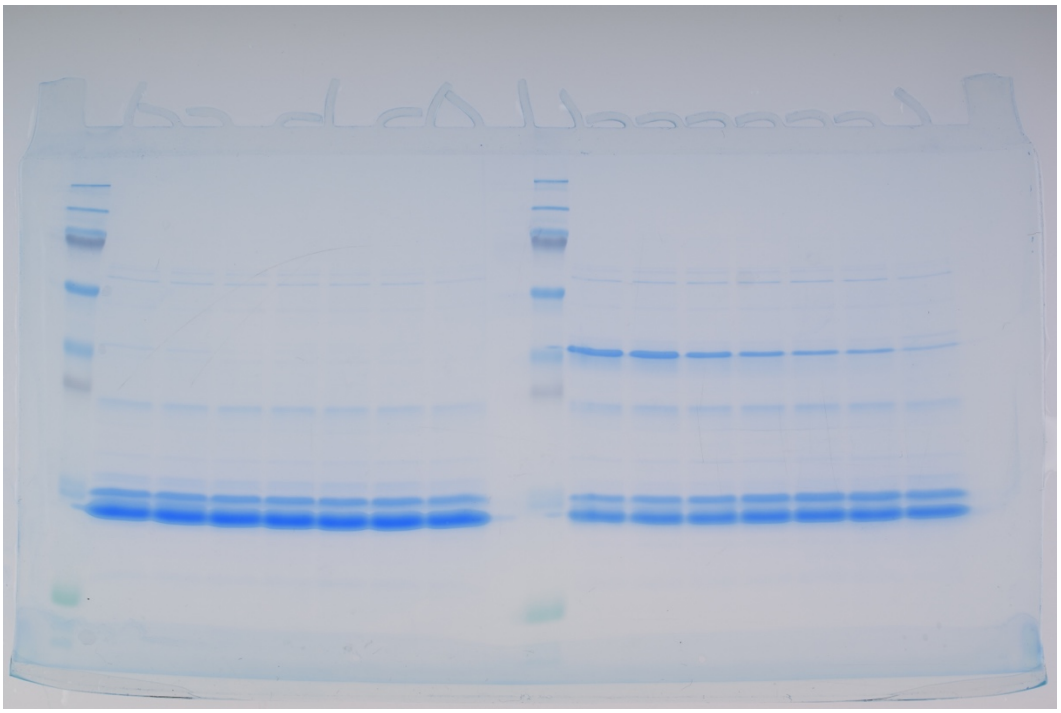

Figure S13.